Dynamics of capacitive Josephson-junction arrays subjected to electromagnetic radiation

Ravi Bhagavatula, C. Ebner, and C. Jayaprakash
Department of Physics, Ohio State University, Columbus, Ohio 43210
(Received 8 July 1991; revised manuscript received 14 October 1991)

We have studied the dynamics of regular two-dimensional Josephson-junction arrays subjected to electromagnetic radiation at frequencies comparable to the individual junction's characteristic frequency. The junctions are described using the resistively-shunted-junction model including capacitance with the plasma frequency also comparable to the characteristic frequency. The dynamical behavior falls into several different general classes, namely, periodic, quasiperiodic, and chaotic, depending on the particular characteristics of the junctions, the input currents, and the amplitude and frequency of the radiation. Detailed examples of each of these types of behavior are given. Current-voltage characteristics are examined and related to the dynamical behavior and the junction's properties. The effect of finite temperatures, included by means of a Langevin noise current, is also discussed, as is the stability of various types of dynamical states.

I. INTRODUCTION

The dynamical behavior of Josephson-junction arrays has been studied in considerable detail, both experimentally[1–4] and theoretically.[5–10] Emphasis in recent theoretical work has centered on the dynamics in the presence of an applied static magnetic field and in the limit of zero-junction capacitance so that the junctions are overdamped. An exception, and the work most closely related to our research, is Ref. 10 in which the types of dynamical states and their stability are studied for a linear series array of junctions with capacitance.

In this paper we present some results from an extensive and continuing study of the dynamics of regular two-dimensional Josephson-junction arrays on a square lattice in the presence of an incident electromagnetic (rf) field and applied dc bias currents. A finite junction capacitance is included. Our intention is to give a broad survey of the possible behaviors of the arrays; more detailed exploration of particular types of states will be given separately. Our study is motivated, in part, by the possibility[1,11] of constructing detectors or generators of microwave radiation from arrays. A second, more theoretical, motivation is the possibility of observing dynamical e.g., chaotic and quasiperiodic, behavior of an unusual sort in these nonlinear, continuous time, coupled systems. We focus on the character of the locally stable modes of oscillation given different input currents and incident rf fields for arrays with various characteristic parameters. Numerous similar investigations have been performed for a single capacitive Josephson junction.[12,13] Also, for use as detectors, an important measure of the response of the system is the mean voltage across the array and its variation with changes in the rf field incident radiation. Consequently, we also present typical I-V curves for the arrays and relate the characteristics of these curves to the dynamical states.

Section II of the paper contains descriptions of the model employed for the array, the numerical methods used for its analysis, and the quantities studied; Sec. III is devoted to presentation of the numerical results while Sec. IV is given to a linear stability analysis of certain dynamical modes; a discussion and summary compose Sec. V.

II. MODEL AND METHODS OF ANALYSIS

We describe a Josephson junction using the resistively-shunted-junction (RSJ) model[14] including the junction capacitance and noise. The essence of this model is that the current through a junction between two superconductors is written as a sum of several kinds of currents in parallel. These include a displacement current I_D through a capacitance C; a normal or quasiparticle current I_N through a resistance R; a supercurrent (the Josephson current) I_S; and a fluctuation or noise current I_F. Thus, the total current in the junction is

$$I = I_D + I_N + I_S + I_F \ . \tag{1}$$

The displacement and normal currents may be expressed in terms of the voltage V across the junction,

$$I_D = C\frac{dV}{dt}$$

and (2)

$$I_N = \frac{V}{R} \ .$$

The supercurrent is expressed as a function of the superconducting phase difference ϕ across the junction

$$I_S = I_c \sin\phi \ , \tag{3}$$

where I_c is the critical current. Further, the relation between the voltage and phase is

$$V = \frac{\hbar}{2e}\frac{d\phi}{dt} \ . \tag{4}$$

Finite temperatures can be introduced by means of I_F which is taken to be a Langevin noise current representing random quasiparticle currents tunneling through the junction. This current is given the properties

$$\langle I_F(t)\rangle = 0$$

and

$$\langle I_F(t+t')I_F(t)\rangle = \frac{2kT}{R}\delta(t') , \tag{5}$$

where the brackets $\langle \cdots \rangle$ denote an ensemble average; T is the temperature and k is Boltzmann's constant.

Combining these relations and dividing by the critical current, one finds that the current in the junction can be written as

$$i \equiv \frac{I}{I_c} = \left[\frac{C\hbar}{2eI_c}\right]\frac{d^2\phi}{dt^2} + \left[\frac{\hbar}{2eRI_c}\right]\frac{d\phi}{dt} + \sin\phi + i_F(t) , \tag{6}$$

where $i_F \equiv I_F/I_c$. Notice that, from Eq. (5),

$$\langle i_F(t+t')i_F(t)\rangle = \sigma\delta(t') \tag{7}$$

with $\sigma = 2kT/RI_c^2$.

Introduce the junction's characteristic frequency $\omega_c \equiv 2eRI_c/\hbar$ and plasma frequency $\omega_p \equiv \sqrt{2eI_c/C\hbar}$; also, introduce a dimension-free time $\tau = \omega_p t$. Then the current may be written as

$$i = \frac{d^2\phi}{d\tau^2} + \beta_c^{-1/2}\frac{d\phi}{d\tau} + \sin\phi + i_F , \tag{8}$$

where $\beta_c \equiv (\omega_c/\omega_p)^2$. Equation (8) is the basic equation of motion for the RSJ model of a capacitive junction.

Given an array of junctions meeting at a set of superconducting nodes k, one can write the RSJ equation for an individual junction in terms of the difference of the phases of the superconducting order parameters on the individual nodes. We assume a uniform array, meaning that all junctions have the same parameters ω_p, ω_c, and I_c. The equation for the current in the junction between neighboring nodes k and l is

$$i_{kl} = \frac{d^2\phi_k}{d\tau^2} - \frac{d^2\phi_l}{d\tau^2} + \beta_c^{-1/2}\left[\frac{d\phi_k}{d\tau} - \frac{d\phi_l}{d\tau}\right] + \sin(\phi_k - \phi_l) + (i_F)_{kl} . \tag{9}$$

We further assume the nodes are sufficiently small that the phase of a node is spatially uniform and that charging effects on a node are negligible so that the sum of the currents entering a given node is zero. This condition determines how the equations of motion of the various junctions are coupled,

$$\sum_{l\in\nu(k)} i_{kl} = -(i_e)_k , \tag{10}$$

where the sum is over those neighbors l of k which are coupled to it by junctions, and $(i_e)_k$ is the input current, in units of I_c, to the kth node from external sources.

Equations (9) and (10) are the equations of motion for the array. Given some initial conditions on the phases and their time derivatives, a set of input currents, and a formulation of the fluctuation currents, they present a well-defined dynamical problem involving the solution of a set of coupled, second-order, ordinary, nonlinear differential equations. They may be expressed in matrix form[15] as

$$G\left[\frac{d^2\phi}{d\tau^2} + \beta_c^{-1/2}\frac{d\phi}{d\tau}\right] = -\sin\phi - i_F - i_e , \tag{11}$$

where G is a matrix and ϕ, $\sin\phi$, i_F, and i_e represent, respectively, vectors comprising the ϕ_k's, $\sin\phi_k$'s, $(i_F)_k$'s, and $(i_e)_k$'s. The elements of G are

$$G_{kl} = \begin{cases} n_k & \text{if } l = k \text{ and } n_k \text{ is the number of junctions entering node } k, \\ -1 & \text{if } k \neq 1 \text{ and } k \text{ and } l \text{ are joined by a junction,} \\ 0 & \text{otherwise .} \end{cases} \tag{12}$$

For any given G, the inverse can be obtained numerically. There is however, one technical point that should be mentioned. If there are N nodes, then there are N equations. The matrix G for this set of equations possesses no inverse, a fact that can be related to overall current conservation, meaning that the net current entering the array must be zero, and to the fact that the system is invariant under a shift of the phases of all of the nodes. We can arbitrarily set the phase of one node equal to a constant, thereby reducing the number of independent variables and the number of equations by one. The matrix G for the remaining $N-1$ equations possesses an inverse which is easy to compute. Given this matrix, we recast the equations of motion as

$$\frac{d^2\phi}{d\tau^2} + \beta_c^{-1/2}\frac{d\phi}{d\tau} = G^{-1}(-\sin\phi - i_F + i_e) . \tag{13}$$

This form is more amenable to efficient numerical solution than the original one.

We turn now to the inclusion of incident electromagnetic fields. A static applied magnetic induction and incident electromagnetic radiation may be described by means of vector potentials $\mathbf{A}_s$ and $\mathbf{A}_{rf}$. The coupling to the array is introduced by replacing the phase difference in the Josephson current $\phi_k - \phi_l$ with $\phi_k - \phi_l - A(k,l)$, where

$$A(k,l) = \frac{2\pi}{\Phi_0}\int_k^l d\mathbf{l}\cdot\mathbf{A}, \tag{14}$$

Φ_0 is the flux quantum $hc/2e$. In the case of the radiation field, we are interested in microwave frequencies. The corresponding wavelength, or distance over which the vector potential varies appreciably, is on the order of a centimeter. We will suppose that this is much larger than the size of the array and so shall approximate the vector potential at all points on the array by that at its center, in effect making the dipole approximation. Thus, we employ, for a monochromatic wave of frequency ω_r such as may be obtained in a resonant cavity,

$$\mathbf{A}_{\rm rf}(t)=\mathbf{A}_0\sin\omega_r t=\mathbf{A}_0\sin\beta_r^{1/2}\tau\ , \tag{15}$$

where $\beta_r=(\omega_r/\omega_p)^2$. For this case,

$$A(k,l)=\frac{2\pi}{\Phi_0}\mathbf{A}_0\cdot(\mathbf{r}_k-\mathbf{r}_l)\ . \tag{16}$$

Given an ordered array such that the nodes are on the sites of a regular lattice, and with junctions only between nearest-neighbor sites, the $A(k,l)$ are the same for all junctions oriented in a particular direction.

Because of the special character of $A(k,l)$ in the dipole approximation, a change of variables can be made to remove all reference to the vector potential from the terms representing the Josephson currents. Define

$$\phi_k'\equiv\phi_k+\frac{2\pi}{\Phi_0}\mathbf{A}_0\cdot\mathbf{r}_k\sin(\beta_r^{1/2}\tau)\ . \tag{17}$$

In terms of this variable, the current in a junction between nodes k,l may be written, with a shift in the origin of the time variable, as

$$\begin{aligned} i_{kl}=&\frac{d^2\phi_k'}{d\tau^2}-\frac{d^2\phi_l'}{d\tau^2}+\beta_c^{-1/2}\left[\frac{d\phi_k'}{d\tau}-\frac{d\phi_l'}{d\tau}\right]\\ &+\sin(\phi_k'-\phi_l')+i_F\\ &+\frac{2\pi}{\Phi_0}\mathbf{A}_0\cdot(\mathbf{r}_k-\mathbf{r}_l)\sqrt{\beta_r^2+\beta_r\beta_c^{-1}}\sin(\beta_r^{1/2}\tau)\ . \end{aligned} \tag{18}$$

An applied uniform static magnetic induction $\mathbf{B}_s$ can be included by adding a simple vector potential, e.g., $\mathbf{A}_s=(\mathbf{B}_s\times\mathbf{r})/2$. Then the $A(k,l)$'s will depend on the positions of the sites (k,l) and a transformation of the phases will not result in simplification of the equations of motion.

In the work described in Sec. III, we employ $M\times M$ arrays on a square lattice, as shown schematically in Fig. 1, with a distance a between nodes. For definiteness, let the array lie in the $z=0$ plane with the x direction along the side of the lattice of length Na and the Y direction along the side of length Ma. We identify a node with two indices (i,j), where $i=1,2,\ldots,N$ and $j=1,2,\ldots,M$. We apply input currents along the opposite edges $i=1$ and $i=N$. These currents may be functions of j. Total current conservation is implemented by extracting the same total current from one edge as is injected at the opposite edge. Along the two lateral edges of the array, given by $j=1$ to $j=M$, we allow no current to enter or leave the system.

Because of the orientation of the array, only the x and y components of the vector potential will enter the equations of motion. For an applied rf field, and in the dipole approximation, we choose

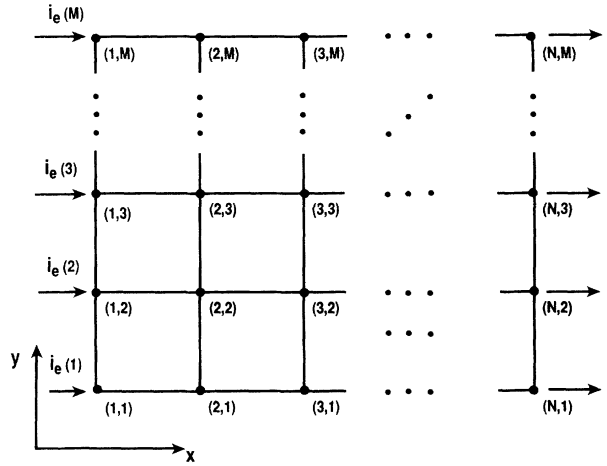

FIG. 1. Schematic diagram of a $N\times M$ array. The nodes are represented by discs with the i and j values of a node shown in parentheses. The junctions are represented by solid lines. Input currents are also shown.

$$\mathbf{A}_{\rm rf}=A_0(\cos\alpha\hat{\mathbf{x}}+\sin\alpha\hat{\mathbf{y}})\sin(\beta_r^{1/2}\tau)\ , \tag{19}$$

α is the angle between $\mathbf{A}_{\rm rf}$ in the x-y plane and the x direction. Then, from Eq. (16),

$$A_{\rm rf}(i,j;i+1,j)=\frac{2\pi a}{\Phi_0}A_0\cos\alpha\sin(\beta_r^{1/2}\tau) \tag{20}$$

and

$$A_{\rm rf}(i,j;i,j+1)=\frac{2\pi a}{\Phi_0}A_0\sin\alpha\sin(\beta_r^{1/2}\tau)\ . \tag{21}$$

When the transformation Eq. (17) is made to the variables ϕ', we find that this vector potential is equivalent to an ac input current along the edges of the array given by

$$\begin{aligned} i_{\rm rf}(1,j)&=\frac{2\pi A_0 a\cos\alpha}{\Phi_0}\sqrt{\beta_r^2+\beta_r\beta_c^{-1}}\sin(\beta_r^{1/2}\tau)\\ &=-i_{\rm rf}(N,j)\equiv i_{rx}\sin(\beta_r^{1/2}\tau) \end{aligned} \tag{22}$$

and

$$\begin{aligned} i_{\rm rf}(i,1)&=\frac{2\pi A_0 a\sin\alpha}{\Phi_0}\sqrt{\beta_r^2+\beta_r\beta_c^{-1}}\sin(\beta_r^{1/2}\tau)\\ &=-i_{\rm rf}(i,M)\equiv i_{ry}\sin(\beta_r^{1/2}\tau)\ . \end{aligned} \tag{23}$$

These equations serve to define i_{rx} and i_{ry}. Note that both of these contributions apply at the corners of the array.

The total input current to the array we take as the rf currents $i_{\rm rf}$ of Eqs. (22) and (23) and dc currents i_e introduced in Eq. (10). Hence, the "external" currents appearing in the equations of motion, Eq. (11) or Eq. (13), become

$$i_e'\equiv i_e+i_{\rm rf} \tag{24}$$

when ϕ is replaced by ϕ'.

III. CALCULATIONS AND RESULTS

Our numerical procedure is to integrate Eq. (13) using a fourth-order Runge-Kutta method. This general technique, but without including the junctions' capacitance, has been used by numerous other workers[6–9] to solve for the behavior of arrays. The step size in time is typically chosen to be around 0.02 of the smallest of the three periods $2\pi/\omega_p$, $2\pi/\omega_c$, and $2\pi/\omega_r$. Smaller step sizes are frequently employed to check the accuracy of the results. Runs lasting anywhere from 10 to several thousand such periods are generally sufficient to determine the character of the asymptotic behavior of the array and to obtain reliably such properties as phase-space trajectories and Fourier transforms of the voltage or supercurrent across individual junctions or the entire array. The array size used in calculations is routinely 8×8, but arrays of size, e.g., 32×32 or 16×64 have been analyzed to examine specific features and to check for size dependence. The properties discussed in this paper tend to be quite insensitive to the size once it is 8×8 or larger. In practice, we measure times in units of the period of the applied rf field; that is, we employ the time variable

$$\tau_r \equiv \frac{\omega_r}{2\pi} t \ . \tag{25}$$

Also, we express time derivatives using this unit of time, defining

$$\dot{\phi}' \equiv \frac{d\phi'}{d\tau_r} = \frac{2\pi}{\omega_r}\frac{d\phi'}{dt} \ . \tag{26}$$

Similarly, frequencies are measured in units of ω_r.

There are numerous parameters entering the equations of motion. These include β_c, β_r, $\mathbf{A}_0$, σ, and the various dc input currents. We have focused attention on the regime where the three frequencies are comparable ($\beta_c \sim 1$ and $\beta_r \sim 1$) and where the dc input currents and effective rf input current are comparable to the critical current, $i_e \sim 1$ and $i_{rx} \sim 1$; $\mathbf{A}_0$ is taken parallel to the x direction so that $i_{ry}=0$. We first studied the dynamical behavior in the absence of noise currents ($T=0$) and then added noise to determine whether any significant changes in the dynamical states occur over and above simple fluctuations superposed on the $T=0$ motion. In the following we first present representative results with applied dc currents and effective rf currents at zero temperature ($i_F=0$) with no static applied field. We then address the effect of finite temperatures.

We have evaluated and analyzed both detailed and global dynamical properties of arrays. These include the time-dependent supercurrents and normal currents, or voltages, in individual junctions and their time averages; time-dependent voltages across the entire array and their time averages (yielding I-V characteristics); and the configuration and motions of vortices. Also, in the case of chaotic states, the character of the chaos and its onset have been studied in some detail. In this paper we do not discuss the motion of the vortices or the properties of the chaotic states.

A. Zero temperature: $i_F=0$

We describe the rf field in terms of the equivalent input currents i_{rx}. As stated earlier, we suppose that $i_{ry}=0$, meaning that the array is oriented with the x direction parallel to the vector potential, or the electric field, of the incident radiation. Finally, for the most part, we take the dc input current in the nodes $(1,j)$ to be uniform along the y direction (independent of j) and given by the single number i_e. Then the parameters of the system in the absence of noise are i_e, i_{rx}, β_c, and β_r. For various sets of these parameters we solve for the motion starting from random initial conditions.

For many parameter sets, the junctions' motions decouple in the sense that, at long enough times, there are no currents in any junctions oriented along the y, or transverse direction. Thus, there are simply independent lines of current along the x, or longitudinal direction. For this type of motion, one need not study a two-dimensional array to determine the dynamical properties. The shapes and locations of the regions in parameter space where decoupled states appear are usually rather irregular. For example, Fig. 2(a) shows points on a grid in i_e-i_{rx} space where the motion did not decouple in computer runs for times up to $2000\pi/\omega_r$ with $\beta_c=1$ and $\beta_r=1$. In these runs, i_e and i_{rx} were set equal to multiples of 0.05 from 0.0 and 2.0 and the system was started from a random configuration of ϕ's and $\dot{\phi}$''s. It should be emphasized that, for some of the points at which the motion did not decouple in our runs, it would have decoupled if we had run a (much) longer time. Also, the amount of time necessary for the system to settle into a decoupled state depends, in some cases quite strongly, on the initial conditions. Indeed, there are instances, as in the case of a single junction,[13] where the character of the long-time state depends on the initial conditions because there are numerous locally stable states of motion. This behavior tends to be especially true, not surprisingly, if the parameters are such that the system is close to a boundary between regions of predominantly coupled and predominantly decoupled states. Hence, the figure should be interpreted as meaning that, where there is a point, the system is likely to remain in a coupled state for a long time if started with random initial conditions; there may be, but need not be, one or more locally stable decoupled states for the same parameters. Similarly, where there is no point in the figure, that means the system is likely to remain in a decoupled state at long times, although there may be locally stable coupled states.

The regions where the motion decouples depend strongly on β_c and β_r. General trends are somewhat elusive. One might expect that, if $\beta_c \sim 1$ so that $\omega_c \sim \omega_p$, then the long-time dynamical state is more likely to be decoupled if ω_r is either much larger or much smaller than the other frequencies, i.e., $\beta_r \gg 1$ or $\beta_r \ll 1$. This expectation is borne out to some extent. For example, using the same grid as employed to obtain Fig. 2(a) we found a small number—about 25—of coupled states at long times with $\beta_c=4$ and with either $\beta_r=25$ or $\beta_r=\frac{1}{25}$. In these two cases the locations of the coupled states are distributed quite differently. For $\beta_r=25$ they are widely

spread in i_{rx} but all close to $i_e=0.7$, whereas for $\beta_r=\frac{1}{25}$, they are dispersed at relatively large i_{rx} and small i_e, implying that there is no simple rule for the probable locations of coupled or decoupled states.

Another trend we have found is the following: if the capacitance, or β_c, is small, so that the displacement current is not important and the system is overdamped, then too the dynamical state will be decoupled. Then, as β_c increases, more coupled states can be expected. For example, in Fig. 2(b), we show the regions of coupled states for $\beta_c=1$ and $\beta_r=25$. In contrast to the results for the same β_r and $\beta_c=4$, we find a large region where coupled states appear at long times. For further contrast, we show in Fig. 2(c) the behavior for $\beta_c=4$ and $\beta_r=\pi^2/25$ which demonstrates that the distribution of coupled states can be quite complex.

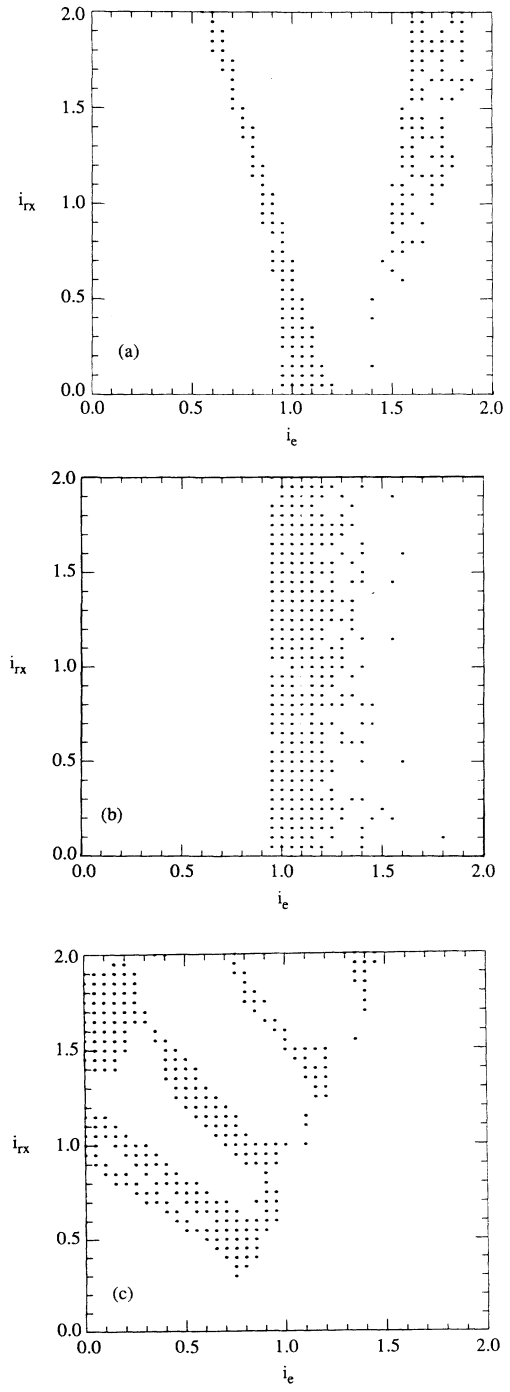

FIG. 2. Points on a grid with spacing 0.05 in the space of i_e and i_{rx} at which coupled long-time dynamical states are found for (a) $\beta_c=\beta_r=1$, (b) $\beta_c=1$ and $\beta_r=25$, and (c) $\beta_c=4$ and $\beta_r=\pi^2/25$. Arrays measuring 8×8 were used to obtain these results as well as those in all of the figures that follow.

To summarize, all cases shown give decoupled states if the input currents i_e and i_{rx} are small compared to unity and also if i_e is significantly larger than unity. Our general findings are that, when started from some random configuration, the arrays show long-time behavior in which the currents either travel straight through the array, so-called decoupled states, or travel in irregular paths so that there are sizable currents in the transverse junctions, so-called coupled states. If β_c, β_r, i_e, and i_{rx} are of order unity, it is difficult to predict, in general, which type of behavior will be observed in the absence of detailed numerical study of that particular case. However, in some instances the behavior is already determined from knowledge of the dynamics of a single junction having the same ω_c and ω_p and driven with the same input currents. For example, if the single junction shows chaotic behavior, so will the array and a coupled state will result.

It is worth commenting on the behavior should the input currents $i_e(j)$ not be independent of j, which is likely to be the case for a real tray. We have done studies with the individual currents $i_e(j)$ varied by random amounts $\delta i_e(j)$ relative to a given mean value i_{e0}, employing $\delta i_e(j)$ as large as 0.5. Then the currents in the array cannot fully decouple into a set of parallel line currents. Rather, states which would be decoupled for uniform inputs tend to show transverse currents on the order of the variation $\delta i_e(j)$ at the edges where the input and output take place; these transverse currents decay toward the center of the array. We find this to be the case even for large $\delta i_e(j)$, relative to the distance from a boundary between the decoupled and coupled dynamical states, indicating that the qualitative response of the array is quite stable against nonuniformities in the inputs. An example is provided by arrays corresponding to Fig. 2(c) with $i_{rx}=1.0$. using $i_{e0}=0.32$, which is less than 0.02 above a region of coupled dynamical states, we find that, even with variations of the individual input currents as large as 0.5, the dynamics remains effectively decoupled and periodic with the transverse currents becoming small in the center of the array; for an 8×8 array, these currents are already smaller at the center than at the edges by an order of magnitude. We have studied this effect by computing the mean value of the absolute current through transverse junctions in larger arrays and find that it decreases exponentially with the distance from the end ($i=1$) of the array. For an array with $M=8$, the decay length is on the order of $2\frac{1}{2}$ junction spacings. This length is, somewhat surprisingly, quite insensitive to β_c, β_r, i_{e0}, or i_{rx}. It is, in fact, a size effect and is proportional to the array

width M. Hence, our conclusion is that, for a sufficiently long (large-N) array, the global character of the long-time stable state is quite insensitive to nonuniformities in the dc bias current; rather, it depends, very sensitively, on the total input current.

We give next a more detailed description of the character of the different possible types of dynamical states, coupled and decoupled, including representative examples of each kind of behavior. The decoupled states, by current conservation, must be such that the currents in all of the longitudinal junctions are the same at all times. If one looks separately at the supercurrent and normal current or voltage, however, one finds that in some instances these are the same in all junctions in the line at a given time and in other instances they are not. In the former case, the array is simply a coherent superposition of single junctions and we refer to the dynamical state as a "single-junction" state; it is also known[16] as a phase-locked state. In the latter case, the supercurrents and voltages in different junctions in the line are the same, but they are shifted in time relative to one another. We have given the name "chain states" to dynamical states of this kind; they are also found in one-dimensional arrays where they are known[16] as antiphase solutions. Note, however, that the existence of such states in two-dimensional arrays is, at first sight, quite remarkable; in spite of the fact that the phase differences across two adjacent junctions in a longitudinal chain do not vary with time in the same way, no current or phase difference is produced across any transverse junction.

For the single-junction or phase-locked states, we find, for all parameter sets investigated, that the period is

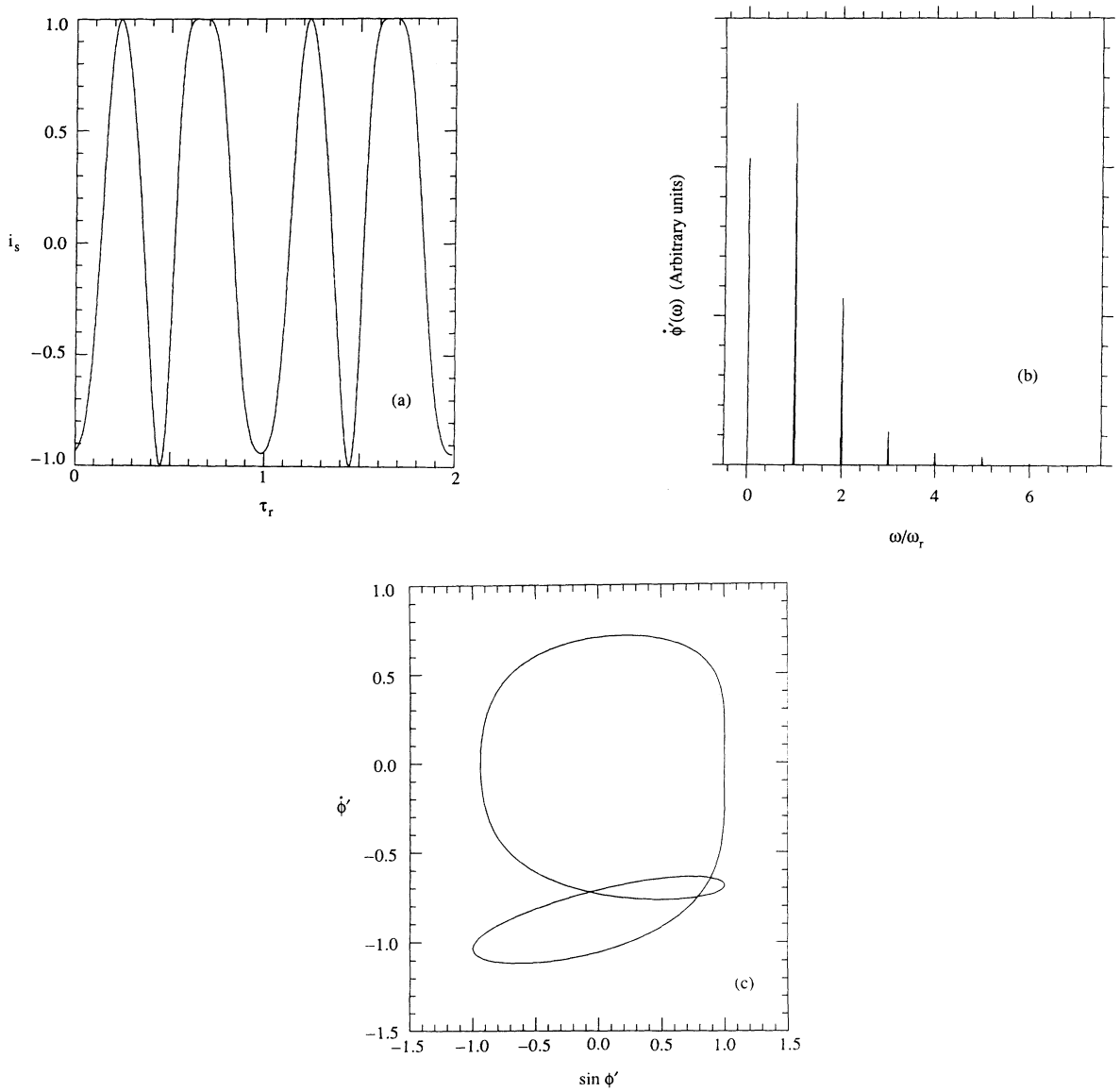

FIG. 3. For a single-junction state at $\beta_c=4$, $\beta_r=\pi^2/25$, $i_{rx}=1.0$, and $i_e=0.4$, we show for a longitudinal junction (a) the supercurrent as a function of τ_r, (b) the power spectrum of $\dot{\phi}'$, and (c) the phase-space trajectory ($\dot{\phi}'$ vs ϕ'). All longitudinal junctions are equivalent in this state.

equal to the period of rf field or to some integral multiple of it. As an example of this type of behavior, we present in Fig. 3(a) the supercurrent, Fig. 3(b) the Fourier transform or power spectrum of $\dot{\phi}'$, and Fig. 3(c) the phase-space trajectory $\dot{\phi}'$ versus $\sin\phi'$ for a longitudinal junction in an array with $\beta_c=4$, $\beta_r=\pi^2/25$, $i_e=0.4$, and $i_{rx}=1.0$; cf., Fig. 2(c). There is no mistaking the simple periodic character of the motion with a period of $2\pi/\omega_r$. If one increases i_e, leaving other parameters the same, period doubling is observed at $i_e\approx 0.59$, and again at 0.64; there is further period doubling followed by the onset of chaotic behavior—and a coupled dynamical state—around $i_e=0.66$. Similarly, if one decreases i_e, a coupled dynamical state is found to appear by the time i_e has reached 0.30. Much the same behavior appears in a single junction[17] with the same parameters, except, of course, the chaotic states involve a single junction.

As an example of a chain state, we present in Fig. 4(a) the supercurrent, Fig. 4(b) the power spectrum of $\dot{\phi}'$, and Fig. 4(c) the phase-space trajectory for a longitudinal junction in the interior of an array with $\beta_c=4$, $\beta_r=\pi^2/25$, $i_e=1.8$, and $i_{rx}=1.0$. Insofar as we can tell, the motion is not precisely periodic. If it is periodic, the period is much larger than the period of the driving field. This is a characteristic property of chain states in general. The power spectrum shows large apparently sharp peaks at frequencies ω/ω_r equal to 1.704, 2.704, etc.; the widths of these peaks are smaller than the resolution of our calculation. There are smaller sharp peaks at integral values of ω/ω_r. Finally, there are much smaller peaks at,

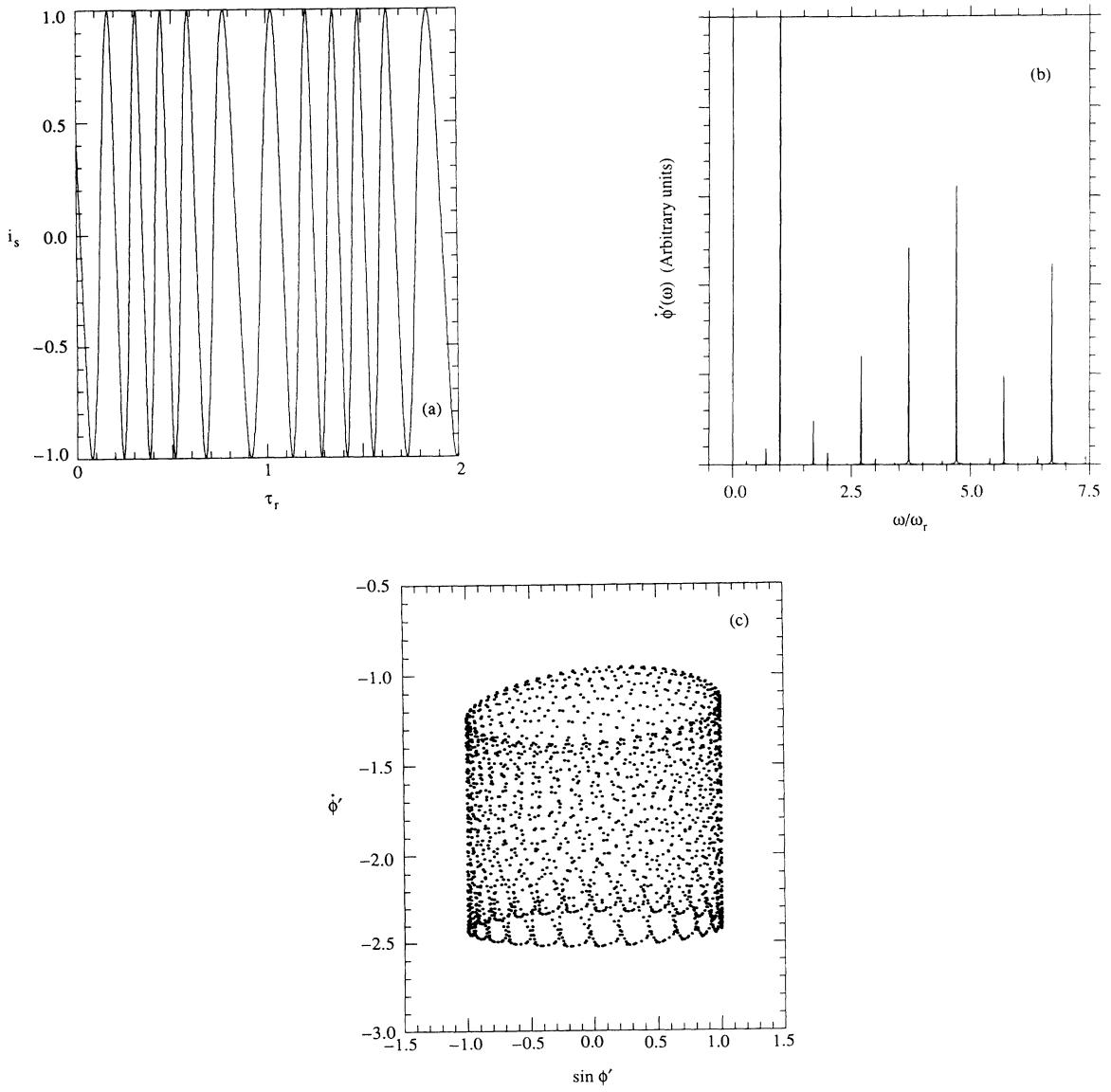

FIG. 4. For a chain state at $\beta_c=4$, $\beta_r=\pi^2/25$, $i_{rx}=1.0$, and $i_e=1.8$, we show for the longitudinal junction between nodes (4,4) and (5,4) (a) the supercurrent as a function of τ_r, (b) the power spectrum of $\dot{\phi}'$, and (c) the phase-space trajectory. The last of these, as well as all phase-space trajectories in the following figures, is discrete, the points being at intervals of the step size used when integrating the equations of motion.

e.g., $(1-0.704)$, $(1+2\times0.704)$, and $(1+3\times0.704)$, which suggests that there are two basic frequencies of motion, one of which is certainly ω_r and the other of which is around $0.704\omega_r$. The system generates frequency components which are various linear combinations of these basic frequencies. If the two frequencies are incommensurate, then the motion is not truly periodic. Similar behavior is observed for other chain states; that is, the power spectrum has sharp peaks at integral values of ω/ω_r and also at one or more sets of additional frequencies displaced from the former set by fixed amounts which do not appear, in general, to be commensurate with the driving frequency ω_r. Furthermore, as the junctions' parameters and input currents are varied, the second basic frequency also varies, apparently smoothly.

As stated above, a general feature of the chain states is that the supercurrents or normal currents in different junctions along a longitudinal chain are the same but shifted in time from one another. We have found, by starting the system with judiciously chosen initial conditions, that locally stable dynamical states are obtained in which this time shift is a multiple of the driving period $2\pi/\omega_r$. We conjecture that all locally stable chain states have this property but have not been able to verify our conjecture in the case of dynamical states obtained from random initial conditions. In any event, the basin of attraction for any given chain state is small in that the time shifts of the different junctions depends sensitively on the initial conditions. The basic motion of any given junction, however, does not. Also, an individual chain state is typically easily disrupted with a small perturbation to the system in that the time shifts change as a result of such a

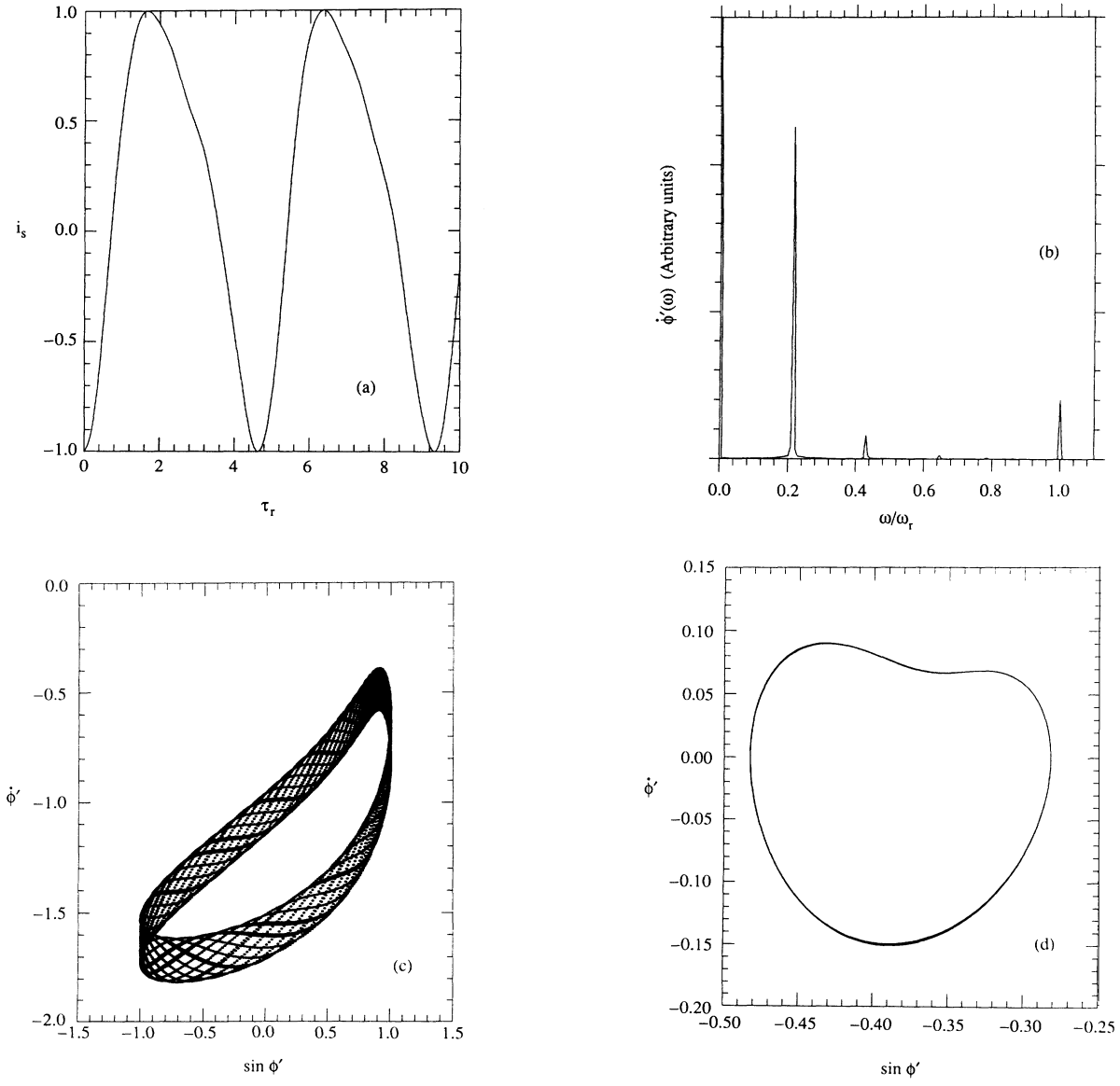

FIG. 5. For a quasiperiodic coupled state at $\beta_c=1$, $\beta_r=25$, $i_{rx}=0.5$, and $i_e=1.25$, we show (a) the supercurrent as a function of τ_r in the longitudinal junction between nodes (4,4) and (5,4), (b) the power spectrum of $\dot{\phi}'$ in the same junction, (c) the phase-space trajectory for this junction, and (d) the phase-space trajectory for the transverse junction between nodes (4,4) and (4,5).

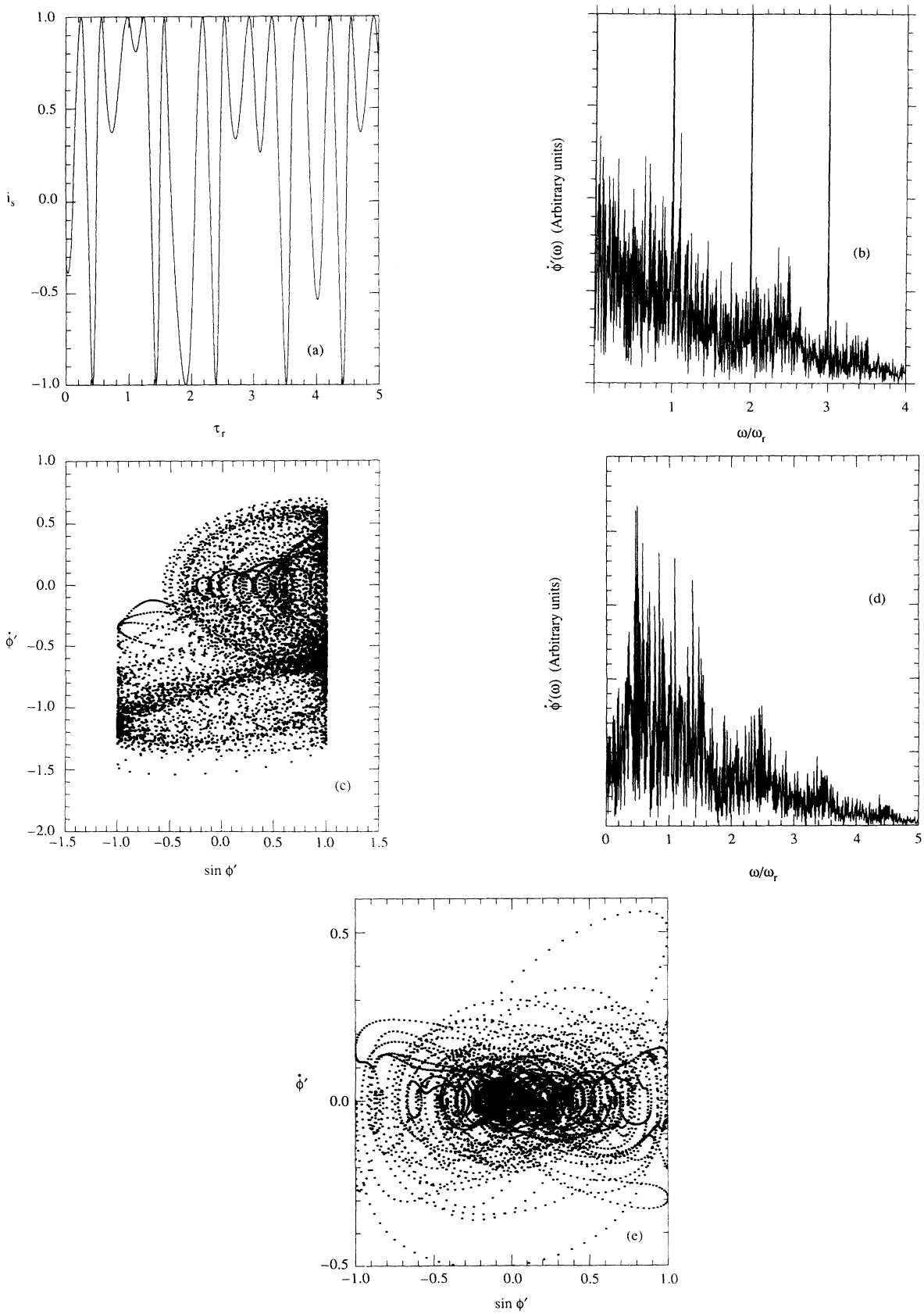

FIG. 6. For a chaotic state at $\beta_c=4$, $\beta_r=\pi^2/25$, $i_{rx}=1.0$, and $i_e=0.69$, we show (a) the supercurrent as a function of τ_r in the longitudinal junction between nodes (4,4) and (5,4), (b) the power spectrum of $\dot{\phi}'$ in the same junction, (c) the phase-space trajectory for this junction, (d) the power spectrum of the neighboring transverse junction between nodes (4,4) and (5,4), and (e) the phase-space trajectory for that transverse junction.

perturbation. Further properties of these states, such as their stability, will be addressed in a separate publication.

As for the coupled states, we have examined the motions for many different parameter sets and have seen just three qualitatively different types of long-time behavior, these being periodic, quasiperiodic, and chaotic. The first of these have periods which are integral multiples of $2\pi/\omega_r$. For example, at $\beta_c=4$, $\beta_r=\pi^2/25$, $i_e=1.235$, and $i_{rx}=1.0$, there is a coupled periodic state with period $5(2\pi/\omega_r)$. These periodic states also have, in general, some spatial periodicity which is typically two junction spacings. In any given state this pattern may be repeated throughout the array or may be only local with different periodic (in space) states present in different parts of the array. Finally, the coupled periodic state tend not to be very robust, meaning that they usually have relatively small basins of attraction and are not found for most sets of initial conditions. Rather, in those places where these states can appear, there is usually a more robust periodic decoupled state.

An example of a coupled quasiperiodic state is provided by an array with $\beta_c=1$, $\beta_r=25$, $i_e=1.25$, and $i_{rx}=0.5$. Figure 5(a) shows the supercurrent in a typical longitudinal junction in the interior of the array; Fig. 5(b) displays the power spectrum of $\dot{\phi}'$ for the same junction; and Figs. 5(c) and 5(d) present, respectively, the phase-space trajectories for this junction and for an adjacent transverse junction. In addition to peaks at integral multiples of the driving frequency, there is a pronounced peak at a frequency close to, but not precisely equal to, $\omega_p=\omega_c=0.2\omega_r$. Further, there are smaller peaks at harmonics of this one's frequency. These peaks are narrower than the resolution of our Fourier transform. As was the case for the chain states, the motion appears to be quasiperiodic rather than truly periodic.

A clear contrast to Fig. 5 is shown by Fig. 6 where we plot in Fig. 6(a) the supercurrent in a longitudinal junction, Fig. 6(b) the power spectrum of $\dot{\phi}'$ in that junction, Fig. 6(c) the phase-space trajectory for the same junction, Fig. 6(d) the power spectrum of a neighboring transverse junction, and Fig. 6(e) the phase-space trajectory for that transverse junction, in an array with $\beta_c=4$, $\beta_r=\pi^2/25$, $i_e=0.69$, and $i_{rx}=1.0$. This is a chaotic state as is demonstrated by the power spectrum and the phase-space trajectories. The power spectrum also shows sharp peaks at harmonics of the driving frequency; these are absent from the power spectrum for a transverse junction.

For applications, one is interested not so much in the behavior of individual junctions in the array, but rather in global properties, in particular, the current-voltage characteristics. In Fig. 7(a) we display the time-averaged mean voltage across an 8×8 array as a function of i_e. The parameters for this system are $\beta_c=4$, $\beta_r=\pi^2/25$, and $i_{rx}=1.0$. The curve shows a number of voltage plateaus or Shapiro steps where the mean voltage is independent of the input current. In these regions the dynamical states are the decoupled states with single-junction behavior; compare Fig. 2(c). There is a wide plateau for $0.31\leq i_e\leq0.65$ and smaller ones in other regions including many at small i_e, as in the case of a single junction,[13] which are two narrow to appear in the figure. There are no plateaus for i_e larger than about 1.5, although this is a region where the dynamical states are decoupled. These states are, however, chain states rather than single-junction states. Floquet analysis, similar to that done in Ref. 10, demonstrates that the single-junction states are unstable here. As a rule, chain states correspond to regions where the voltage varies with i_e. Figure 7(b) shows, for contrast, the I-V curve for a single junction with the same parameters as used for Fig. 7(a). The structure of the curve is similar but with more pronounced voltage variations. Also, of course, the voltage is seven times larger for the array.

These I-V curves may be contrasted with what is found if the capacitance is zero, $\omega_p\rightarrow\infty$. In that case, there is a sequence of wide, evenly spaced voltage plateaus for currents up through and well beyond what is shown in

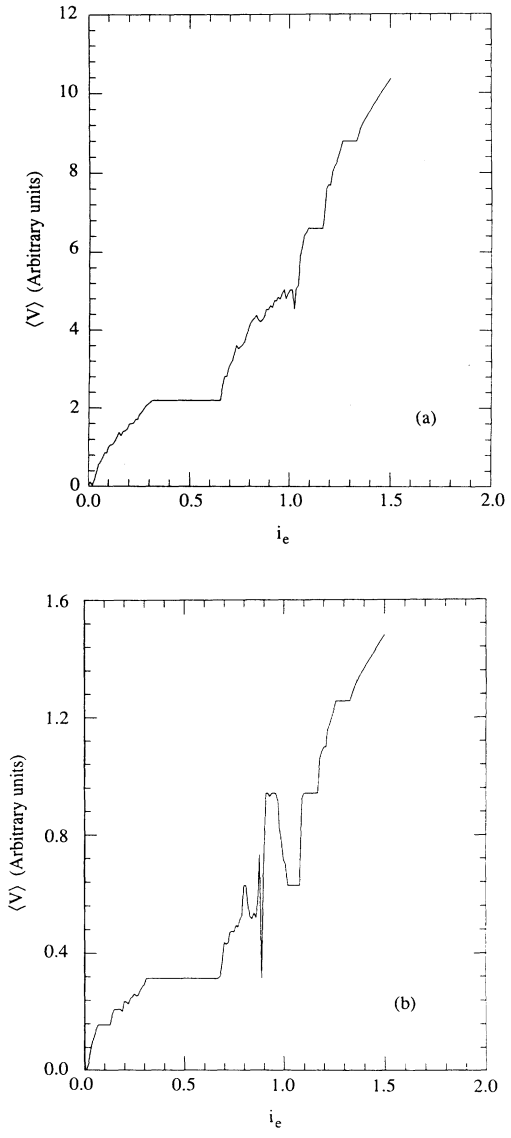

FIG. 7. For $\beta_c=4$, $\beta_r=\pi^2/25$, and $i_{rx}=1.0$, we show the I-V curves for (a) an 8×8 array and (b) a single junction. The voltages on corresponding plateaus are seven times larger for the array than for the single junction.

the figures. Hence, we can conclude that the addition of capacitance to the junctions in this instance suppresses the higher Shapiro steps, at least for the dynamical behavior at the times which we investigated. At the same time, the edges of the remaining steps tended to become sharper with the addition of the capacitance, reflecting the fact that the presence of capacitance does not, in general, result in an overall degradation of the steps, as has been demonstrated also by others.[12,18] In the present example, as described above, there is just one wide plateau remaining with a number of narrower ones which do not necessarily occur at voltages that are integral multiples or simple fractions of the voltage of the wide one (which is at the same voltage as the first step produced by an array with negligible capacitance).

In the regions between plateaus, where the voltage typically increases with i_e, the dynamical state is either a chain state or a coupled state. Specifically, at relatively large i_e, $i_e \sim 1.5$ and above, it is the chain state that is present while for i_e in the region below about 1.0, there are chaotic states. Thus there is a simple correspondence of decoupled, periodic dynamical states with the voltage plateaus and either coupled states or aperiodic decoupled states with the regions where the voltage changes with input current. Similar statements apply in this case of a single junction; there are periodic states on the voltage plateaus and either chaotic or quasiperiodic states elsewhere.

We have studied the transition from periodic to chaotic behavior in some detail. As an example, we cite the transitions as one moves from the large plateau in Fig. 7(a) either upward or downward in i_e into chaotic regimes. In the former case, there is a sequence of period doubling transitions with increasing i_e until chaotic behavior sets in around $i_e = 0.66$, a standard route to chaos. The behavior for decreasing i_e is not the same. In this case we find no period doubling. Rather, the power spectrum, which is necessarily initially a set of perfectly sharp peaks at integral multiples of ω_r, evolves by developing widths in the peaks accompanied by the gradual appearance of a noisy background at all frequencies. Hence, two quite different routes to chaos appear in this one example.

It is appropriate to compare the behavior of the array with that of a single junction having the same characteristics. In many respects the two are comparable. That is, the single junction also displays periodic, quasiperiodic, and chaotic behavior. Of course, with a single junction one cannot observe coupled as opposed to decoupled dynamical states. Roughly speaking, the regimes where the array shows coupled chaotic states are also ones where the single junction is chaotic; where the array displays periodic behavior, the single junction is also periodic with the same period, and where the array shows aperiodic but decoupled behavior, the single junction is also aperiodic. It is, however, sometimes difficult to make a detailed comparison. As a rule, if the single junction is chaotic then the array is; there are some regions where the array is apparently chaotic but the single junction is not. This observation may be a consequence of the finite times we are able to follow the motions of the array. That is, it is not inconceivable that in some of these cases the array would exhibit long-time periodic or quasiperiodic behavior were we able to follow it long enough. Consider as an example junctions with $\beta_c = 4$, $\beta_r = \pi^2/25$, and $i_{rx} = 1.0$. For i_e between 0.07 and 0.13, there is a region, corresponding to the voltage plateau in Fig. 7(b), where the single junction is periodic. At many values of i_e in this range we found, for 8×8 arrays, chaotic rather than periodic behavior starting from randomly selected initial states.

B. Effects of noise

The addition of noise currents to the system provides a means by which it may escape from one locally stable

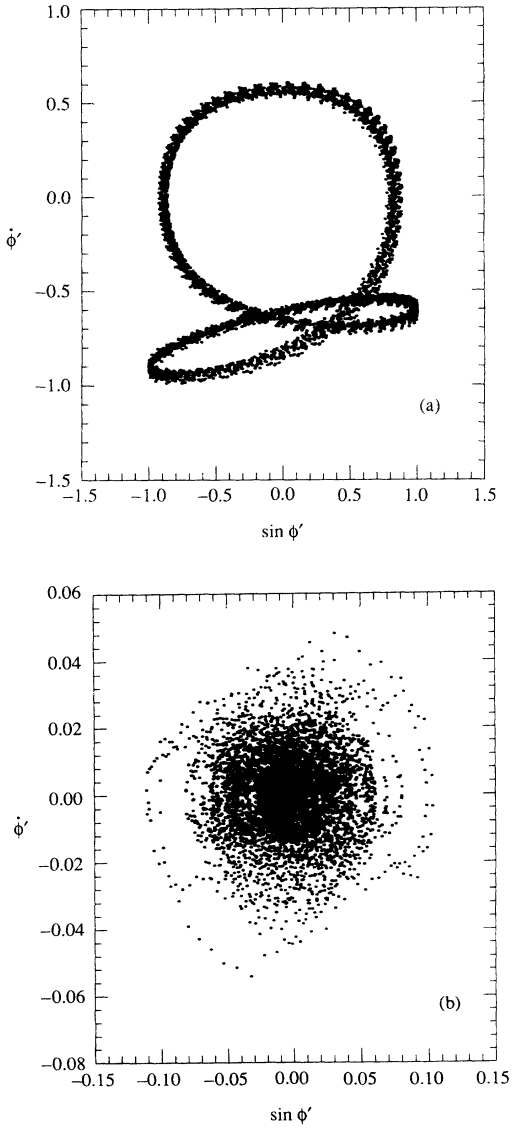

FIG. 8. The phase-space trajectory for (a) the longitudinal junction between nodes (4,4) and (5,4) and (b) the transverse current in the junction between nodes (4,4) and (4,5), for $\beta_c = 4$, $\beta_r = \pi^2/25$, $i_{rx} = 1.0$, $i_e = 0.32$, and $|i_F| \leq 0.4$.

dynamical state to another. Further, the characters of various types of states must change somewhat; specifically, the decoupled states are no longer truly decoupled because fluctuating currents must appear in the transverse junctions. In addition, periodic states are no longer truly periodic because of the noise. The most interesting question associated with the presence of noise is whether states are destabilized by it.

One well-known[19] consequence of the noise is that the edges of the plateaus in the current-voltage plot become rounded. Small plateaus are lost altogether. Purely periodic states become quasiperiodic in that the power spectrum still has sharp peaks with some background present. The phase-space trajectories demonstrate the quasiperiodic behavior very vividly; Fig. 8, which may be compared with Fig. 3(c), is for $\beta_c=4$, $\beta_r=\pi^2/25$, $i_{rx}=1.0$, and $i_e=0.32$, with the rather large noise current[20] $|i_F(t)|\leq 0.4$. Even this large fluctuating current is not sufficient to disrupt the basic periodic state; notice, however, that in the absence of noise, if i_e were reduced to 0.30, a reduction of just 0.02, a chaotic state would result. The periodic unperturbed state is evidently quite robust against noise, even as it is robust against nonuniform input currents.

Comparably large noise currents also do not destroy other types of unperturbed states. We mention, in particular, the chain states which maintain their basic character, described above, in the presence of the noise.

IV. STABILITY ANALYSIS

From Sec. II, the condition of current conservation at node k may be expressed as, for $i_F=0$,

$$\sum_{l\in\nu(k)}\left[\frac{d^2}{d\tau^2}+\beta_c^{-1/2}\frac{d}{d\tau}\right](\phi'_k-\phi'_l)+\sin(\phi'_k-\phi'_l)+i'_e(k)=0\ . \quad (27)$$

In the following, we shall specify a node using indices i,j as in Sec. II, $\phi'_k(\tau)\rightarrow\phi'(i,j;\tau)$.

We begin by considering the stability of the single-junction states. These are characterized by a single-phase function $\phi_0(\tau)$. If we let the phases of the individual nodes in the single-junction state be designated as $\phi'_0(i,j;\tau)$, then these are related by

$$\phi'_0(i,j;\tau)-\phi'_0(i',j';\tau)=(i-i')\phi_0(\tau)\ . \quad (28)$$

To test this mode's stability, we write $\phi'(i,j;\tau)$ as

$$\phi'(i,j;\tau)=\phi'_0(i,j;\tau)+\psi(i,j;\tau)\ , \quad (29)$$

and expand Eq. (27) in powers of ψ, keeping just linear terms,

$$\left[\frac{d^2}{d\tau^2}+\beta_c^{-1/2}\frac{d}{d\tau}\right][4\psi(i,j)-\psi(i+1,j)-\psi(i-1,j)-\psi(i,j+1)-\psi(i,j-1)]+\cos\phi_0[2\psi(i,j)-\psi(i+1,j)-\psi(i-1,j)]+[2\psi(i,j)-\psi(i,j+1)-\psi(i,j-1)]=0\ . \quad (30)$$

Finally, we Fourier transform the linearized equations of motion in space, making use of the fact that the nodes are on a square lattice with spacing a, and obtain

$$\frac{d^2\psi(\mathbf{q};\tau)}{d\tau^2}+\beta_c^{-1/2}\frac{d\psi(\mathbf{q};\tau)}{d\tau}+f[\mathbf{q};\phi_0(\tau)]\psi(\mathbf{q};\tau)=0\ , \quad (31)$$

where

$$f\equiv\frac{(1-\cos q_x a)\cos\phi_0+(1-\cos q_y a)}{2-\cos q_x a-\cos q_y a}\ . \quad (32)$$

In the single-junction mode, $\cos[\phi_0(\tau)]$ is periodic, and as a consequence $f(\mathbf{q},\tau)$ is also periodic so that Floquet theory[21] may be applied. First, note that, for $|q_x|<|q_y|$, $f(\mathbf{q},\tau)>0$ for all τ. Consequently, the uniform solution is stable against perturbations which satisfy this condition on $\mathbf{q}$. More generally, we convert the second-order equation (31) to a pair of first-order equations by introducing

$$x_1(\tau)=\psi(\tau)$$

and

$$x_2=\frac{d\psi(\tau)}{d\tau}\equiv\psi'\ , \quad (33)$$

so that

$$x'_1=x_2 \quad (34)$$

and

$$x'_2=-\beta_c^{-1/2}x_2-fx_1\ ,$$

or, in matrix form,

$$x'=Ax\ , \quad (35)$$

where

$$x=\begin{bmatrix}x_1\\x_2\end{bmatrix}$$

and

$$A=\begin{bmatrix}0 & 1\\ -f(\tau) & -\beta_c^{-1/2}\end{bmatrix}\ . \quad (36)$$

We have analyzed these equations, finding, in particular, the two characteristic multipliers α_i for a variety of single-junction states. In all cases examined we find that the absolute values $|\alpha_i|$ are less than unity for any finite q_y. However, one of them is very close to unity for q_y small. The implication[21] is that the periodic uniform states are (locally) asymptotically stable, although the decay time of a perturbation can be very long. These predictions are supported by our numerical results; all periodic uniform states that we have encountered have proved to be locally stable.

Next, suppose that $\cos[\phi_0(\tau)]$ is chaotic corresponding to a decoupled uniform state in which each junction undergoes the same chaotic motion. In this case the uniform solution is one in which the entire system behaves like a single junction and exhibits uniform global chaos. We may argue, however, that this state is unstable with respect to small perturbations. Suppose a phase at one node is perturbed relative to its value in the uniform state. This disturbance will grow as a consequence of the state being a chaotic one with a positive Liapunov exponent. Further, the disturbance will spread to the nearby nodes, which are coupled to the original one, and so will grow in spatial extent as time progresses as well as growing on each node where it is present; hence, the uniform state is unstable. This conclusion is also supported by our numerical results. All chaotic states that we have studied show short-ranged spatial correlations in the chaotic part of the motion. However, the chaotic fluctuations tend to be accompanied by some underlying periodic motion with longer-ranged correlations.

V. DISCUSSION AND SUMMARY

We have studied the dynamical states of two-dimensional arrays of capacitive Josephson junctions with dc bias and an applied monochromatic rf field using the RSJ model. For wide ranges of junction parameters, we find stable or metastable solutions of several basic types. First, the states are either coupled, meaning that there are currents in junctions perpendicular to the input currents, or decoupled, meaning that the input currents pass straight through the array, producing no currents in the transverse direction. In the latter case, the arrays display either single-junction (phase-locked) states or chain states in which the junctions in a longitudinal chain all behave in the same fashion but successive junctions in the chain are time shifted by apparently random multiples of the period of the rf field. At the same time, the states of parallel junctions in different chains are identical so that the system is invariant under translation in the transverse direction.

Also, both kinds of decoupled states are generally very robust in that random changes in the initial conditions do not often lead to a different dynamical state at long times; in the case of the chain state, such a perturbation typically produces a different chain state in that the amounts by which different junctions are time shifted relative to each other change. Similarly, thermal noise, included by means of a Langevin noise current in each junction, does not easily destabilize these states although it does, of course, cause them to fluctuate around some mean properties. Similarly, random variations in the input currents do not have significant effects on the decoupled states so long as the total input current is unchanged. In the latter case, there are produced currents in transverse junctions close to the nodes where the current is injected, but these die out exponentially with distance with a decay length on the order of one-half of the array's transverse length.

The rather impressive stability of the dynamical modes against thermal noise and disorder in the inputs is somewhat surprising. It would be useful to know also whether the dynamical states are as stable when there is configurational disorder in the array; we intend to study this question and report on it separately. We do not at this point have an explanation for this stability. Nevertheless, it is encouraging in that it implies that reliable devices such as rf radiation detectors could be constructed from junction arrays.

The coupled dynamical states are either periodic, quasiperiodic, or chaotic. The periodic states that we found to be uncommon in that they have relatively small basins of attraction and do not appear very often if the simulation is started with random initial conditions. More commonly, for those parameters where these states can appear, a periodic decoupled state usually is the result of starting from an arbitrarily chosen configuration. The periodic states are interesting in that they also display spatial periodicity. As for the quasiperiodic states, these behave in time rather like the chain states but have, in addition, currents in the transverse junctions. Finally, chaotic states are quite common; we have found that chaos can appear by a sequence of bifurcations during which the array is in a single-junction state and also by intermittency.

The current-voltage characteristics of the array have been examined and correlated with the dynamical states. There are voltage plateaus where the voltage remains constant for some range of i_e or i_{rx}. The dynamical states on these plateaus are single-junction states or periodic coupled states. Off the plateaus one finds coupled and chain states. The presence of capacitance in the arrays tends to suppress the plateaus and produce fairly smooth variation of the voltage with the input currents, especially in the region of relatively large i_e (larger than about 1.5) where predominantly chain states are found. For smaller i_e and with $i_{rx} \sim 1$, chaotic states are not common off the voltage plateaus. Also, in this region there are numerous very small plateaus. Overall, the behavior of the I-V curves is not unlike that for a single junction with the same properties as the junctions in the array, although much of the detail of the curve for the single junction is lost.

Of the various phenomena we have found, several seem worthy of further investigation. These include the detailed character of the chaos in this extended, continuous-time system, the rather remarkable stability of the various dynamical states, especially the decoupled ones, to different kinds of noise and disorder, and certain features of the chain states. Further work on these and other aspects of the dynamics of capacitive arrays is in progress.

ACKNOWLEDGMENTS

This work was supported in part by the Air Force Office of Scientific Research through Grant No. AFOSR-89-0527. One of us (C.J.) acknowledges support from the Department of Energy, DOE, Office of Basic Energy Sciences, Grant No. DE-FG02-88ER13916. The simulations were done using the Ohio Supercomputer Center Cray Y-MP8/864. Use of the Ohio State University Department of Physics VAX 8650 is also acknowledged.

[1]S. P. Benz and C. J. Burroughs, Appl. Phys. Lett. **58**, 2162 (1991).

[2]S. P. Benz, M. S. Rzchowski, M. Tinkham, and C. J. Lobb, Phys. Rev. Lett. **64**, 693 (1990).

[3]D. W. Abraham, C. J. Lobb, M. Tinkham, and T. M. Klapwijk, Phys. Rev. B **26**, 5268 (1982).

[4]R. F. Voss and R. A. Webb, Phys. Rev. B **25**, 3446 (1982).

[5]K. H. Lee, D. Stroud, and J. S. Chung, Phys. Rev. Lett. **64**, 962 (1990).

[6]J. U. Free, S. P. Benz, M. S. Rzchowski, M. Tinkham, C. J. Lobb, and M. Octavio, Phys. Rev. B **41**, 7267 (1990).

[7]K. K. Mon and S. Teitel, Phys. Rev. Lett. **62**, 673 (1989).

[8]W. Xia and P. L. Leath, Phys. Rev. Lett. **63**, 1428 (1989).

[9]J. S. Chung, K. H. Lee, and D. Stroud, Phys. Rev. B **40**, 6570 (1989).

[10]P. Hadley, M. R. Beasley, and K. Wiesenfeld, Phys. Rev. B **38**, 8712 (1988).

[11]D. R. Tilley, Phys. Lett. **33A**, 205 (1970).

[12]R. L. Kautz and R. Monaco, J. Appl. Phys. **57**, 875 (1985), and references therein.

[13]M. Iansiti, Q. Hu, R. M. Westervelt, and M. Tinkham, Phys. Rev. Lett. **55**, 746 (1985).

[14]See, e.g., K. K. Likharev, *Dynamics of Josephson Junctions and Circuits* (Gordon and Breach, New York, 1986).

[15]S. R. Shenoy, J. Phys. C **18**, 5163 (1985).

[16]See, e.g., P. Hadley, M. R. Beasley, and K. Wiesenfeld, Phys. Rev. B **38**, 8712 (1988).

[17]See also M. Iansiti, Q. Hu, R. M. Westervelt, and M. Tinkham, Phys. Rev. Lett. **55**, 746 (1985), where single junctions, with somewhat different parameters, are studied.

[18]M. Levi, Phys. Rev. A **37**, 927 (1988).

[19]See, e.g., J. S. Chung, K. H. Lee, and D. Stroud, Phys. Rev. B **40**, 6570 (1989).

[20]In the interest of numerical efficiency we have used noise currents distributed uniformly on the stated intervals, rather than ones with Gaussian distributions which would be more appropriate for thermal noise. Tests using a Gaussian distribution demonstrate that our results are not sensitive to this distinction. More generally, one should also be sensitive to the question of the frequency of sampling which is done here at intervals of the basic time step used for solving the equations of motion. Comparison of results with different time steps did not yield any qualitative differences. These points are discussed by J. Voss, J. Low Temp. Phys. **42**, 151 (1981).

[21]For a description of linear stability theory for the solutions of ordinary differential equations, see, e.g., R. Grimshaw, *Nonlinear Ordinary Differential Equations* (Blackwell, Oxford, 1990), Chaps. 3 and 4.